Published in final edited form as:
J Magn Reson Imaging. 2011 November ; 34(5): 1159–1166. doi:10.1002/jmri.22715.

MRI-Guided Vascular Access with an Active Visualization Needle

Christina E. Saikus, B.S., **Kanishka Ratnayaka, M.D.**, **Israel M. Barbash, M.D.**, **Jessica H. Colyer, M.D.**, **Ozgur Kocaturk, Ph.D.**, **Anthony Z. Faranesh, Ph.D.**, and **Robert J. Lederman, M.D.**
Cardiovascular and Pulmonary Branch, Division of Intramural Research, National Heart, Lung, and Blood Institute, National Institutes of Health, Bethesda, MD, USA.

Abstract

Purpose—To develop an approach to vascular access under MRI, as a component of comprehensive MRI-guided cardiovascular catheterization and intervention.

Materials and Methods—We attempted jugular vein access in healthy pigs as a model of "difficult" vascular access. Procedures were performed under real-time MRI guidance using reduced field of view imaging. We developed an "active" MRI antenna-needle having an open-lumen, distinct tip appearance and indicators of depth and trajectory, in order to enhance MRI visibility during the procedure. We compared performance of the active needle against an unmodified commercial passively-visualized needle, measured by procedure success among operators with different levels of experience.

Results—MRI-guided central vein access was feasible using both the active needle and the unmodified passive needle. The active needle required less time (88 vs. 244 sec, p=0.022) and fewer needle passes (4.5 vs. 9.1, p=0.028), irrespective of operator experience.

Conclusion—MRI-guided access to central veins is feasible in our animal model. When image guidance is necessary for vascular access, performing this component under MRI will allow wholly MRI-guided catheterization procedures that do not require adjunctive imaging facilities such as X-ray or ultrasound. The active needle design showed enhanced visibility, as expected. These capabilities may permit more complex catheter-based cardiovascular interventional procedures enabled by enhanced image guidance.

Keywords

Interventional MRI; Vascular access; Actively visualized devices

INTRODUCTION

Arterial or venous access is necessary prior to any endovascular procedure and typically accomplished using direct palpation or anatomic landmarks. In difficult cases, such as patients with peripheral vascular atherosclerosis and obesity, adjunctive image guidance with X-ray fluoroscopy or ultrasound can be helpful. Standby X-ray is used frequently to confirm guidewire position before placing large introducer sheaths, especially when tactile feedback suggests an irregularity. Complications can arise from this seemingly simple

Corresponding Author: Robert J. Lederman, M.D. Address: National Institutes of Health, 10 Center Drive, Building 10, 2C713, Bethesda, MD, 20892-1061, Telephone: (301) 402-6769.

Financial Interest
No author has a financial conflict of interest. NHLBI and Siemens have a collaborative research and development agreement covering inteventional cardiovascular MRI.

procedure including vascular injury or mural disruption, hematoma, pseudoaneurysm. arteriovenous fistula, or life-threatening hemorrhage (1). Percutaneous vascular access can also be difficult in research animals such as swine with small or impalpable vessels requiring surgical exposure at some facilities.

The superior soft tissue visualization and multi-planar viewing capabilities of MRI is appealing to guide endovascular and minimally-invasive interventions. Interventional MRI aims to apply these features for procedural guidance to identify anatomic structures, target pathologies and plan optimal approaches. Most devices used to date for interventional MRI are passively visualized. They are typically visible as dark artifacts, or negative contrast, due to water displacement and the different magnetic susceptibilities relative to water, causing small local inhomogenities in the B0 static magnetic field, and radiofrequency (RF) inhomogeneity (2). The device appearance can vary widely with exact material composition, magnet field strength, orientation relative to B0, and imaging sequence (2–4). Active devices aim to produce a unique imaging signature by incorporating small coils or antennae connected to the scanner for device tracking using computer-synthesized markers superimposed on images (5) or simply for visualization (“profiling”) of the device as imaged alongside neighboring tissue.

We are developing real-time MRI guidance for transcatheter procedures (6). Direct percutaneous vascular access inside the interventional MRI system would be an attractive alternative to access in the X-ray system followed by transfer to the MRI system. MRI-guided vessel access could exploit the inherent vessel contrast and greater anatomic context of the vessel and its path.

In a porcine model of difficult vascular access, we evaluated the ability of MRI with narrow field of view to guide needle access to blood vessels. We hypothesized that real-time MRI needle and guidewire access to the jugular vein is feasible, using reduced field-of-view techniques and active profiling needle devices. We developed a custom “active” profiling needle and compared it with commercial “passive” MRI-compatible needles in procedure time and number of passes required for successful access. We also hypothesized that enhanced imaging guidance would enable novice operators to achieve access with proficiency similar to that of more experienced operators.

MATERIALS AND METHODS

Active Needle Design and Construction

The needle design aimed to incorporate active profiling to delineate the tip clearly while maintaining an open-lumen and the desired mechanical properties to allow the device to be used *in vivo* for cardiovascular access applications. An 18-gauge MRI-compatible needle base, initially a commercially available 15cm *Inconel* 625 needle (EZ-EM, Lake Success, NY USA) and then a custom ground Nitinol needle, was modified to incorporate a loop antenna along its length on a separate receiver channel. To provide clear tip location and indication of needle depth and shaft trajectory, tighter copper coil windings around the insulated needle were separated by unequal distances to produce local signal increases at distinct points, starting just proximal to the tip (at the end of the bevel) and at 1, 3, 6, 10 and 15 cm away to provide distinguishable marker points. Thermoplastic elastomer (*Pebax*) covering maintained a smooth transition and profile on the outer surface from needle bevel to coil without a significant increase in outer diameter (<5Fr, 1.67mm) as seen in Figure 1. To enable free movement of the needle, it was connected to its remote tuning and matching circuitry via a 1-meter long coaxial cable extension. The needle was impedance matched to 50 ohms at 63.67 MHz (Larmor frequency for 1.5T), used in receive-only mode, and

detuned during RF transmission with a PIN diode and parallel resonant circuit. The active needle was connected to a separate scanner receiver channel via a preamplifier box.

Imaging

All imaging and interventions were performed in a short, wide bore 1.5T MRI scanner (Espree, Siemens Medical Solutions, Erlangen, Germany) with surface receive coils in addition to the independent active device channels. High resolution phantom images were acquired using a balanced steady-state free precession (bSSFP) sequence (TR/TE 3.92/1.96ms, slice thickness 5mm, flip angle 45°, field of view 340×170mm, matrix 256×128). Real-time bSSFP imaging (TR/TE 3.67/1.23ms, slice thickness 6mm, flip angle 45°, matrix 192×144) used a separate real-time reconstruction and display system (7) and was performed during phantom testing and *in vivo* animal experiments. The active needle signal was displayed as a color overlay on the anatomical grayscale images in the real-time reconstruction system.

In Vitro Needle Imaging Characterization

In vitro testing was conducted in water phantoms under various conditions that may be experienced during *in vivo* use using the sequences described above. To evaluate needle appearance changes during different orientations with respect to B0, the needle was fixed in place at the proximal end within a rectangular phantom that could be aligned parallel and perpendicular to B0. Imaging was also performed with a stylet and guidewire occupying the device lumen to ensure that the active signal was still visible. Signal-to-noise (SNR) maps of the device signal profile were generated using a single magnitude image of the device only channel. The noise was calculated from a user-selected “noise-only” region outside the device and phantom and corrected for the number of active channels (8,9).

To characterize the accuracy of coil visualization in determining needle location, we recorded coil marker appearance along the device and measured tip and centerline deviations. The device centerline and tip location were determined by fixing the needle in a plexiglass holder with small water channels providing MR visible distance markings. Marker locations were determined by the centroid of the marker points after threshold segmentation. The differences between the set tip position and visible tip position and deviation of signal intensity at the tip from the device centerline were calculated.

Vascular Access In vivo

The active needle was evaluated *in vivo* during real-time MRI-guided jugular vein access in swine. Animal experiment protocols were approved by the institutional animal care and use committee, according to contemporary NIH guidelines. Yorkshire farm pigs (mean 36.3 kg ± 7.8 kg) underwent mechanical ventilation with inhaled isoflurane.

Operators—We tested the ability of MRI to allow inexperienced operators to perform difficult vascular access by comparing novice (medical student), intermediate (fellow), and experienced (attending interventional cardiology) operators.

Jugular Vein Access—Jugular vein access in swine was selected as a model of difficult vascular access because pulses are typically not palpable, anatomic and radiographic landmarks are limited, the veins readily spasm when instrumented, and the veins collapse under superficial pressure (10). A total of 30 vessel access procedures were attempted, 17 with the active needle (average vessel size of passive needle attempts 0.80 ± 0.09 cm) and 13 with the passive needle (0.81 ± 0.10 cm). When possible, bilateral jugular vein access was attempted in the same animal by a given operator for comparison of active and passive needle use as described later in this section.

A non-tortuous target segment of vein was selected from a stack of free-breathing T2-weighted scout images, as was a potential entry site and needle trajectory. We used a small 7cm loop coil (Siemens) to reduce the field-of-view, and positioned it inside a sterile bag, adjacent to the needle entry site. This allowed an alias-free field-of-view 229 × 135 mm and in-plane resolution 1.2 × 0.94 mm at 2 frames/second (Figure 2). The interactive real-time MRI guidance system allowed the use of prior 3D MR angiographic roadmap overlays to assist in slice positioning, and also allowed active needles to be used with device-only projection mode to detect out-of-plane device position (7).

To guide needle orientation and advancement, we used two interleaved orthogonal real-time MRI slices along the long-axis of the selected vessel segment (sagittal and coronal oblique), along with an occasional third short-axis slice. The needle entry site was identified on imaging using an MR-conspicuous locator (operator's finger, a syringe containing normal saline or 1% (5 μM) gadopentetate, or an active needle containing saline flush) positioned along the animal neck. The needle entry angle was 30–45° to the skin surface according to standard catheter technique, and needle traversal guided interactively by the real-time MRI slices to enter the target vessel segment. In general, scanning presented the target to the operator, and the needle was adjusted as needed to return into the selected imaging plane. Scan planes were adjusted interactively as needed when the operator or needle displaced the target vessel.

Vessel entry was confirmed by imaging, by gadopentetate 1% angiography, and by successful insertion of a nitinol guidewire (Glidewire .035", Terumo, Somerset, NJ) into the lumen down towards the right atrium. Finally, the needle was exchanged for a standard introducer sheath, securing access to the vessel.

Active and Passive Needle Comparison—Access was attempted bilaterally on a total of 12 of the animals with either the active needle design or the unmodified passively visualized needle, for a total of 24 access attempts. The planning and imaging approach described above was the same for the active and passive needle attempts, other than only the active needle being visible at skin entry with saline flush. To minimize the influence of which needle (active, passive) or side (right, left) the operator started with, operators alternated both the type of device and the side that access was attempted initially.

Endpoints and Statistical Analysis—Needle puncture of the vessel with blood return and advancement of a guidewire for sheath exchange within 15 minutes of skin entry was defined as a *successful vascular access attempt*. Success rates, procedure time and number of passes needed to access the vessel were compared between attempts with the active and passive needles. *Procedure time* was considered from first skin puncture to successful placement of a wire into the vessel. A *needle pass* was defined by an attempted vessel puncture. The time-based success measures were not normally distributed, particularly given procedure failure. Therefore we used non-parametric, unpaired statistical tests (Fisher's Exact Rank for Success Rates and Mann-Whitney U for time and passes) to compare the procedure outcome measures for the active and passive needle attempts. Parameters are reported as mean ± one standard deviation with two-tailed P values reported and < 0.05 considered significant. We did not correct for multiple comparisons.

RESULTS

Active Needle Construction and In vitro Visualization

Needle construction and circuitry produced distinct points of increased signal intensity in phantom images corresponding to the prescribed spacing along the length of the needle. A minimum spacing of 0.5 cm between tightly wound segments provided distinct markers that

could be identified with the device parallel or perpendicular to B0. These points were visible despite changes in needle artifact size and appearance which is seen along with a SNR map in Figure 3. The signal from the needle was also apparent when the needle was used with an accompanying MR-compatible stylet, passive nitinol guidewire, and active guidewire (images not shown).

In quantitative measures of coil positioning and targeting accuracy, the active needle coil started 3.5 mm from the end of the needle bevel which resulted in a difference of 4.2 mm from the centroid of the most distal marker signal to the bevel end. The coils closely represented the true device centerline with centroids that deviated from the actual needle central lumen by less than 0.5 mm (average for distal 3 points: 0.2 mm, range: 0–0.38 mm). The distance between the marker points measured by MRI were within 5% of the actual marker separation (average: 2.35%, range: 0.6–5%).

Jugular Access In vivo

Real-time MR imaging enabled careful selection of the skin and vessel target site and visualization of the vascular access and guidewire placement. Use of a small receive coil at the surface helped maintain the sterile field and allowed reduced field of view imaging without wrap-around artifacts for better visualization of the target vessel during the procedure. Representative procedure images with the skin trajectory and needle access with the active needle are shown in Figure 4.

The needle device performed as expected, allowing blood return, selective angiography, and wire passage through the 0.035”-guidewire-compatible central lumen. Increase in coil signal was also apparent when the vessel was entered, corresponding to the increase in available signal source. The device channel signal profile could extend along the guidewire when it was inserted through the needle lumen and coupled to the needle receive coil.

Operators were marginally more successful in achieving jugular vein access within the allocated 15 minutes using the actively visualized needle than the passive needle. Successful attempts using the active needle were shorter and with fewer needle passes than those using a passive needle. For all access attempts, 12 of 17 (71%) active attempts vs. 8 of 13 (62%) passive attempts were successful, p=0.71. The results for the subset of 12 animals with bilateral access attempted systematically in each animal are shown in Figure 5 where access was achieved in 10 out of 12 animals (83%) with the active approach and 7 of 12 (58%) for the passive, p=0.37. Among successful procedures, average time-to-access was shorter using the active needle (88 vs. 244 sec, p=0.022), and required fewer needle passes (4.5 vs. 9.1, p=0.028). Including all access attempts, and censoring failure attempts as time to access of = 900 sec and number of passes = 15 since rank-based statistics were used, the differences between active and passive approaches for number of passes (p = 0.019) and time to access (p=0.016) remained significant

Operator experience did not have a clear impact on the success or duration of the access procedures although operator subsets were small (Table 1). Results were more variable with the passive needle attempts than active needle ones. In the animals with bilateral attempts, intermediate and advanced operators were successful on all active attempts while the two failures by the novice occurred (1) in the first procedure and then (2) during a later attempt when wire placement was unsuccessful after vessel access (bleedback). Time to access and number of passes in the successful procedures with the active needle also did not correlate with experience and were similar between groups. For passive needle access, the novice operator was more successful and quicker than the intermediate and advanced operators which were more variable. Expert operators provided a subjective report that the MRI-

compatible needles were less sharp, longer, and prone to bending compared with conventional steel x-ray access needles.

DISCUSSION

We developed an active needle with distinct markers of needle position, trajectory and insertion depth. We tested this needle in an animal model of “difficult” vascular access, to support future standalone MRI-guided cardiovascular catheterization. The device construction permitted smooth entry into the skin and maintained the central lumen available for blood return, pressure, aspiration, and guidewire use. The distinct signal and image signature allowed clear device localization during MRI.

We found MRI provided useful information to the operator — including desired vessel entry site, simultaneous multi-planar views, and needle position — not generally available with X-ray or ultrasound. The displayed anatomic context and relative needle position and trajectory enabled operators with little or no experience successfully to achieve vascular access with little or no training. We found continuous long-axis imaging of the needle and target vessel to be most helpful, especially when using the passively-visualized needle, as recommended for ultrasound-guided access (11). Our approach of redirecting a needle based on a fixed anatomic target differs from other posited image-guidance strategies wherein the imaging slice is adjusted automatically based on needle position (12).

Other MRI capabilities may enhance procedure safety and success compared with other standalone modalities. Previously acquired MR angiograms may provide enhanced roadmaps combined with real-time imaging slices in the 3D-visualization window. Extravasation and hematoma are quickly recognized and treated without delay typical of X-ray workflows to administer exogenous contrast. In our experience, we observed one intraprocedural hematoma formation after unsuccessful needle passage but no inadvertent carotid punctures. Soft-tissue imaging can avert needle entry to bystander structures and reduce complications. Selective contrast injection remains an option.

MRI-guided vascular access was accomplished with both actively and passively visualized MRI-compatible needles. When actively or passively visualized needles are perfectly aligned with the imaging plane (Figure 6) the tip position is evident. However, in our experience particularly with a slightly longer (15 cm) and more flexible needle, this was not always the case and accounted for much of the extra time spent and errant passes during the passive needle attempts. The active needle design, in contrast, allowed rapid and clear device localization during the interventional MRI procedures with its distinct imaging markers of needle position, trajectory and insertion depth. Special MRI techniques, such as device-only projection mode, or device-finding snap-to scan-plane prescription, also enhanced usability (7,13).

Other investigators have applied a needle stylet designed with a tip tracking coil in a novel PEEK and ceramic tip construction which was used for targeting liver cysts and MR-guided cholecystostomy (14,15). Tip tracking, however, requires non-imaging tracking MRI pulse sequences where only the tip location and path is marked on prior or interleaved images. In cases where the needle may curve or take trajectories through critical structures, identifying the entire location on simultaneously acquired imaging may be necessary to improve procedure safety. Our device profiling approach incorporates the unique device signature on real-time images. Stylets are less useful in cardiovascular applications where back-bleeding, pressure-monitoring, and ready guidewire access through an open lumen are considered important. The outer coil design provides these features without a significant increase in size or device functionality.

Successful procedures even with the active needle still averaged four passes per attempt where optimally, access would be achieved with a single puncture and entry to the vessel. The needles used were longer and less sharp than typical access needles which where more likely to pass over the vessel and cause spasm without successful puncture. Additionally the needle passive artifact particularly when trajectories perpendicular to B0 are attempted (16) and/or active signal can be relatively large compared to the size of the vessel targeted which could make it more difficult to identify successful vessel puncture. Adequate visualization of the vessel is also critical which can be limited by image spatial and temporal resolution to appreciate vessel location and deformation. Therefore, procedural performance could be improved with enhanced device visualization and mechanical performance and superior vessel imaging.

Alternate non-metallic materials may be superior for artifact reduction but tend to be less sharp and strong. Carbon fiber needle cannulas (14G and 18G) had been commercially available (17) but required an inner metal stylet for puncture. A smaller carbon-fiber-reinforced plastic puncture needle was developed by Fraunhofer Institute for Production Technology (IPT) and is now available in Europe through RadiMed (Germany). The MR visibility of these carbon alternatives, however, may actually be insufficient for our application without modification (18). Newer passive needle designs with specialized coatings have been investigated to provide more precise tip location (19). Several algorithms to better track passively visualized devices including needles also are under development (20) which may assist the procedure with passive devices.

Tip location and targeting accuracy of the active needle may be limited during the procedure by the distance between the start of the coil and the true needle end necessitated by the long bevel and the proximity and distribution of the signal source. Signal visualization can appear larger than the needle size since the coil is on the exterior of the needle base and signal will fall from there which may make targeting small vessels for access more challenging. To further reduce the needle profile, areas to contain the coil winding could include centerless ground depressions in the needle base for the wire. This approach also could position the distal coil closer to the tip. Alternatively, coil windings could detect signal ahead of the actual coil position (21). Non-metallic needle bases as described earlier also could be used to further improve active visualization with less needle base artifact if an appropriately size composite needle becomes available. Finally, different insulative coatings like PTFE or parylene could provide smoother needle passage. Signal can also be lacking in low signal tissues where an internal signal source may be necessary.

Conductive devices like this one create safety and heating concerns. Our design uses cable traps and detuning during RF transmission, to reduce coupling to the high-power RF B1 deposition. However, our design positions these bulky safety elements at needle hub, reducing their effectiveness. Even our short metal needle and coils could interact with the scanner electric field, generating the highest current density and heating at the tip of the needle or coil. It might be possible further to modify the needle coil winding and wire characteristics to reduce induced currents and heating (22,23). Sharp non-metallic needle bases and non-metallic accessory devices like guidewires could improve the safety and limit coupling but currently suffer mechanical limitations and poor visibility. Separate metallic guidewires were associated with enhanced MRI signal, indicating electrical coupling with our needle antenna. This too poses a heating risk at certain insertion lengths, although in our use condition is small because of the relatively central location of the wire inside the bore and animal. In addition to device modifications, scanner and imaging-based approaches are under development that could be used to reduce RF power and E-field coupling (24). That said, in this *in vivo* experience we observed no biological evidence of needle- or guidewire-associated heating such as burn or thrombosis.

Apart from our device enhancement, imaging enhancements might further facilitate this procedure. We reduced the field of view using a small local receive coil. Non-cartesian k-space trajectories like radial or spiral may allow increased temporal resolution to observe vessel deformation and then greater spatial resolution could permit targeting of smaller vessels. The logistics of the MR environment are more complicated than X-ray or ultrasound, but our experience will inform standalone MRI-guided catheterization procedures..

In conclusion, we have demonstrated successful real-time MRI-guided vascular access in swine. Access was achieved with a newly developed active visualization needle and passive comparator using reduced field of view imaging. Compared with a passive needle, the active "profiling" needle had a imaging signature permitted rapid and clear device and tip localization and resulted in higher success rates and shorter procedures. Operator experience did not significantly impact success rate; by contrast, imaging technique and trajectory planning proved important.

MRI-guided vascular access could enable procedures to be performed entirely in the MR suite with greater anatomic information. The active needle design, trajectory planning and real-time MRI guidance also could permit more complex percutaneous cardiovascular interventions where enhanced image guidance is necessary for such procedures to be performed safely.

Acknowledgments

Katherine Lucas, William Schenke and Victor Wright for their assistance with animal experiments.

Grant Support:

Supported by the NHLBI Division of Intramural Research, Z01-HL005062-08 and Z01-HL006041-01

REFERENCES

1. Samal AK, White CJ. Percutaneous management of access site complications. Catheter Cardiovasc Interv. 2002; 57:12–23. [PubMed: 12203921]
2. Ladd ME, Erhart P, Debatin JF, Romanowski BJ, Boesiger P, McKinnon GC. Biopsy needle susceptibility artifacts. Magn Reson Med. 1996; 36:646–651. [PubMed: 8892221]
3. Frahm C, Gehl HB, Melchert UH, Weiss HD. Visualization of magnetic resonance-compatible needles at 1.5 and 0.2 Tesla. Cardiovasc Intervent Radiol. 1996; 19:335–340. [PubMed: 8781155]
4. Lewin JS, Duerk JL, Jain VR, Petersilge CA, Chao CP, Haaga JR. Needle localization in MR-guided biopsy and aspiration: effects of field strength, sequence design, and magnetic field orientation. AJR Am J Roentgenol. 1996; 166:1337–1345. [PubMed: 8633445]
5. Dumoulin CL, Souza SP, Darrow RD. Real-time position monitoring of invasive devices using magnetic resonance. Magn Reson Med. 1993; 29:411–415. [PubMed: 8450752]
6. Saikus CE, Lederman RJ. Interventional cardiovascular magnetic resonance imaging: a new opportunity for image-guided interventions. JACC Cardiovasc Imaging. 2009; 2:1321–1331. [PubMed: 19909937]
7. Guttman MA, Ozturk C, Raval AN, et al. Interventional cardiovascular procedures guided by real-time MR imaging: an interactive interface using multiple slices, adaptive projection modes and live 3D renderings. J Magn Reson Imaging. 2007; 26:1429–1435. [PubMed: 17968897]
8. Constantinides CD, Atalar E, McVeigh ER. Signal-to-noise measurements in magnitude images from NMR phased arrays. Magn Reson Med. 1997; 38:852–857. [PubMed: 9358462]
9. Henkelman RM. Measurement of signal intensities in the presence of noise in MR images. Med Phys. 1985; 12:232–233. [PubMed: 4000083]

10. Swindle, M. Surgery, Anesthesia, and Experimental Techniques in Swine Ames. Iowa: Iowa State University Press; 1998.
11. Kumar A, Chuan A. Ultrasound guided vascular access: efficacy and safety. Best Pract Res Clin Anaesthesiol. 2009; 23:299–311. [PubMed: 19862889]
12. Elgort DR, Wong EY, Hillenbrand CM, Wacker FK, Lewin JS, Duerk JL. Real-time catheter tracking and adaptive imaging. J Magn Reson Imaging. 2003; 18:621–626. [PubMed: 14579407]
13. George AK, Derbyshire JA, Saybasili H, et al. Visualization of active devices and automatic slice repositioning ("SnapTo") for MRI-guided interventions. Magn Reson Med. 63:1070–1079. [PubMed: 20373408]
14. Gohde SC, Pfammatter T, Steiner P, Erhart P, Romanowski BJ, Debatin JF. MR-guided cholecystostomy: assessment of biplanar, real-time needle tracking in three pigs. Cardiovasc Intervent Radiol. 1997; 20:295–299. [PubMed: 9211777]
15. Leung DA, Debatin JF, Wildermuth S, et al. Real-time biplanar needle tracking for interventional MR imaging procedures. Radiology. 1995; 197:485–488. [PubMed: 7480698]
16. Kee ST, Rhee JS, Butts K, et al. Gary J. Becker Young Investigator Award. MR-guided transjugular portosystemic shunt placement in a swine model. J Vasc Interv Radiol. 1999; 10:529–535. 1999. [PubMed: 10357476]
17. Reichenbach JR, Wurdinger S, Pfleiderer SO, Kaiser WA. Comparison of artifacts produced from carbon fiber and titanium alloy needles at 1.5 T MR imaging. J Magn Reson Imaging. 2000; 11:69–74. [PubMed: 10676624]
18. Thomas, C.; Rempp, H.; Springer, F., et al. First performance evaluation of new 3D MRI fluoroscopy system for MRI-guided musculoskeletal interventions in high field. Seventh Interventional MRI Symposium; Baltimore, MD. 2008.
19. Muller-Bierl BM, Martirosian P, Graf H, et al. Biopsy needle tips with markers--MR compatible needles for high-precision needle tip positioning. Med Phys. 2008; 35:2273–2278. [PubMed: 18649458]
20. Koktzoglou I, Li D, Dharmakumar R. Dephased FLAPS for improved visualization of susceptibility-shifted passive devices for real-time interventional MRI. Phys Med Biol. 2007; 52:N277–N286. [PubMed: 17664566]
21. Anderson KJ, Leung G, Dick AJ, Wright GA. Forward-looking intravascular orthogonal-solenoid coil for imaging and guidance in occlusive arterial disease. Magn Reson Med. 2008; 60:489–495. [PubMed: 18666117]
22. Bottomley PA, Kumar A, Edelstein WA, Allen JM, Karmarkar PV. Designing passive MRI-safe implantable conducting leads with electrodes. Med Phys. 37:3828–3843. [PubMed: 20831091]
23. Weiss S, Vernickel P, Schaeffter T, Schulz V, Gleich B. Transmission line for improved RF safety of interventional devices. Magn Reson Med. 2005; 54:182–189. [PubMed: 15968655]
24. Etezadi-Amoli, M.; Stang, P.; Zanchi, MG.; Pauly, JM.; Scott, GC.; Kerr, AB. Controlling induced currents in guidewires using parallel transmit ISMRM. 18th Scientific Meeting & Exhibition; Stockholm, Sweden. 2010.

Figure 1.
Active needle with close up of tip uncovered (top) and covered (bottom).

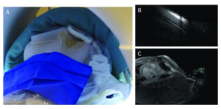

Figure 2.
Access set-up and imaging. (A) Photo of neck access site, prepped with small loop coil in sterile bag. Examples of imaging with (B) and without (C) small loop coil and reduced field of view.

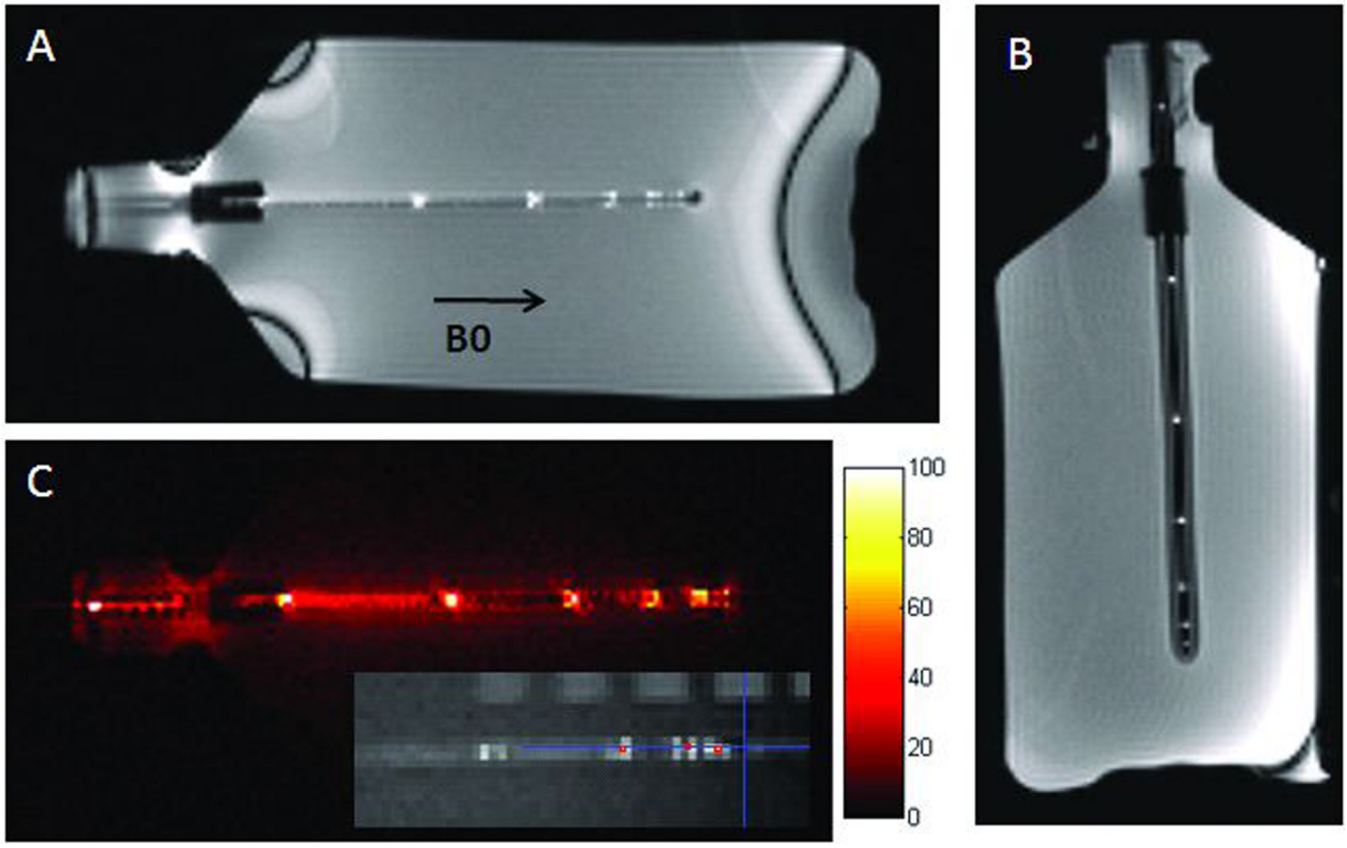

Figure 3.
Active Needle in Phantom. (A) Parallel to B0 and (B) Perpendicular to B0. (C) SNR map for device channel only and sample positioning evaluation (inset).

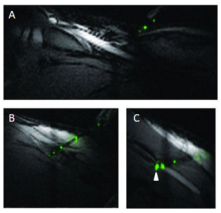

Figure 4.
Active Needle *in vivo*. (A) Planning trajectory with needle on skin surface. (B) Entire needle length and tip location clearly visible. (C) Distal 2 markers seen in vessel.

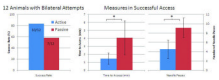

Figure 5.
Access results in 12 animals with bilateral attempts comparing active and passive needles in success rate, time to access, and number of needle passes.

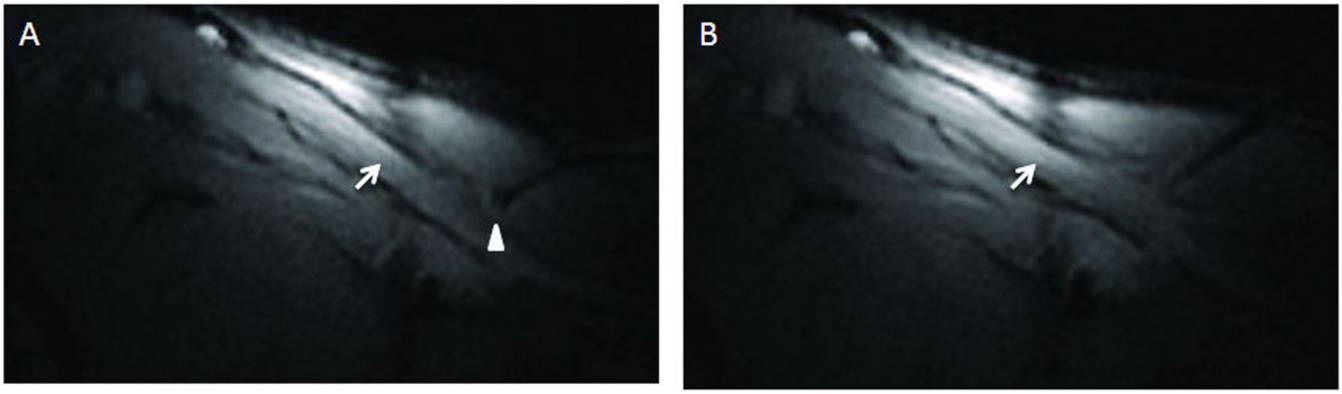

Figure 6.
Passive Needle *in vivo*. Passive needle tip location (indicated by round artifact highlighted with white arrowhead) is visible when aligned in plane (A) but difficult to locate if part of the needle is out of plane (B). Arrow pointing at vessel.

Table 1

Access results comparing novice, intermediate, and experienced operators.

		ACTIVE NEEDLE			PASSIVE NEEDLE		
	n	**Success Rate (%)**	**Passes**	**Time (sec)**	**Success Rate (%)**	**Passes**	**Time (sec)**
Novice	5	60	4.3 ± 1.5	99.0 ± 31.3	80	7.8 ± 3.2	228.3 ± 112.4
Intermediate	3	100	4.0 ± 2.6	94.3 ± 60.1	33	13.0	424.0
Advanced	4	100	4.8 ± 2.6	105.8 ± 54.1	50	13.5 ± 0.70	354.5 ± 98.3